Journal of Cleaner Production 41 (2013) 82–88

Contents lists available at SciVerse ScienceDirect

Journal of Cleaner Production

journal homepage: www.elsevier.com/locate/jclepro

Vision-sensing and bead width control of a single-bead multi-layer part: material and energy savings in GMAW-based rapid manufacturing

Jun Xiong, Guangjun Zhang*, Zhilong Qiu, Yongzhe Li

State Key Laboratory of Advanced Welding and Joining, Harbin Institute of Technology, West Straight Street 92, Harbin 150001, PR China

ARTICLE INFO

Article history:
Received 17 July 2012
Received in revised form
6 October 2012
Accepted 6 October 2012
Available online 17 October 2012

Keywords:
GMAW-based rapid manufacturing
Thin-walled part
Visual sensor
Image processing
Deposited bead width

ABSTRACT

Rapid manufacturing technologies have made it possible to reduce material wastes and to remanufacture valuable dies and tools. This paper focuses on reasonable utilization of materials and energies in gas metal arc welding (GMAW) for rapid manufacturing. During the weld-based additive manufacturing process, geometries of the deposited weld beads should be monitored and controlled. Using a composite filtering technique, a computer vision-sensing system was designed. Features of the weld bead image were analyzed. A corresponding image processing technology was used to extract parameters of the deposited weld beads. An on-line control of the deposited beads was realized based on a segmented neuron self-learning controller. The results show that the proposed control system is capable of keeping the deposited bead width of a thin-walled part consistent, making an efficient use of materials and energies possible.

1. Introduction

In recent years, sustainable manufacturing is a research focus because of the urgency of decreasing material wastes and energy consumptions. Main concerns are related to the design of manufacturing process with the aim of conserving energies and materials or the utilization of the most proper forms for energies and materials (Jovane et al., 2008).

In this circumstance, additive net-shape rapid manufacturing has gained worldwide popularity for its capacity of reducing environmental burdens within materials manufacturing industry (Sutherland et al., 2003). Compared with the traditional removal process in forming components, rapid manufacturing is an additive layered manufacturing process by slicing the 3D geometric model into simple 2.5-dimensional layers (Karunakaran et al., 2010). Significant reductions in production costs and time between the original concept and final product, as well as materials saving are expected with this technique (Santos et al., 2006). By using only the quantity of the material needed, it is capable of decreasing energy consumption and industry scrap compared with conventional fabrication methods. Furthermore, it does not need specifically designed fixture or tooling, increasing the flexibility of the forming process and reducing the cost for fabricating special tools (Morrow et al., 2007).

With an increasing demand for building metallic tools, rapid manufacturing based on GMAW has shown new promises due to advantages of high production efficiency, simple equipment, high density and excellent bonding strength of parts (Mughal et al., 2006).

Generally, the GMAW-based rapid manufacturing process is composed of several procedures including establishment of 3D models of parts, slicing of desired thickness for each layer, design of welding paths and parameters in each layer, and stacking up of deposited weld beads layer by layer. However, the GMAW-based rapid manufacturing process consists of multi-layer depositions. Keeping the heat input as constant, when the number of the deposited beads increases, the deposited weld pool flows easily. The shape of each bead cannot be easily controlled because of serious heat accumulation, especially weld pool located at the boundaries of components. Moreover, bubbles and cavities may generate in the weld pool at high temperature due to an intense metallurgical reaction (Zhang et al., 2003). Thus, the control of heat input is of great importance for increasing the stability in layered deposition process.

At present, most of the works for increasing process stability are based on laser metal deposition (Tang and Landers, 2011; Heralic et al., 2012). To our knowledge little has been focused on the GMAW-based deposition. Several studies have been carried out for

* Corresponding author. Tel./fax: +86 451 86415537.
E-mail address: zhanggj@hit.edu.cn (G. Zhang).

0959-6526/$ – see front matter © 2012 Elsevier Ltd. All rights reserved.
http://dx.doi.org/10.1016/j.jclepro.2012.10.009

the control of heat input during the GMAW-based deposition process. Simple temperature control techniques were developed to decrease the heat input by means of an infra-red remote sensor (Spencer et al., 1998). The deposition did not resume until the part had cooled sufficiently. A projected spray transfer mode was established at low currents by wire electrode oscillation, enhancing the surface quality of weld beads for overlay cladding process (Wu and Kovacevic, 2002; Zhang and Li, 2001; Zhang et al., 1998). On the other hand, a novel hybrid approach, integrating GMAW as an additive and computer numerical control (CNC) milling as a subtractive technique, was developed to improve the surface quality and accuracy of solid freeform fabrication (SFF) parts (Suryakumar et al., 2011; Song and Park, 2006). Each layer was face milled by the CNC machining for removing scallops and stack up of errors, which resulted in material wastes and inefficiency of the process. Nevertheless, the essence of these approaches is an open-loop control.

This research aims at the reduction of material wastes and heat input consumptions during the layered deposition process. An on-line monitoring and control of the process was established through a passive vision-sensing system. The feasibility of the control system was evaluated through deposition of single-pass multi-layer thin walls. Section 2 presents the description of methods. Results and discussion are presented in Section 3. The last Section 4 ends the paper with some main conclusions.

2. Methods

2.1. Experimental system

2.1.1. The functional structure of GMAW-based rapid manufacturing system

The GMAW-based rapid manufacturing system is shown in Fig. 1, which included a three-dimensional welding flat (WF), a welding power supply (WPS), and a computer for sensing and control (CSC). The CSC was the key of the subsystem. It mainly realized three functions: control of the WPS and WF with a USB2813 data acquisition card, control of the vision-sensing system by means of an image acquisition card, and providing human–machine interface consisting of an image displaying and processing module, an arc on/off model, and a model for adjusting welding parameters.

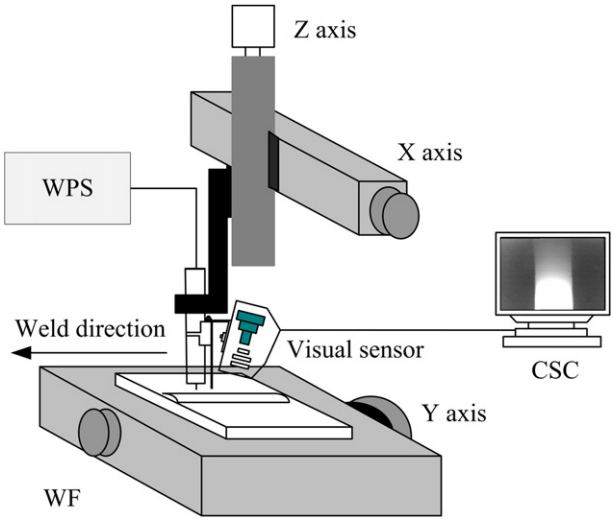

Fig. 1. The schematic diagram of GMAW-based rapid manufacturing system.

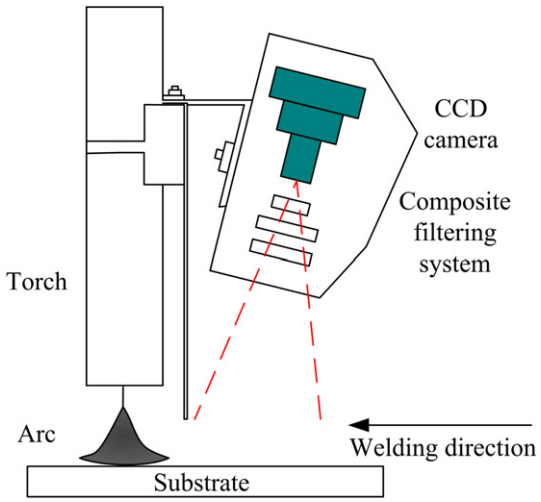

Fig. 2. Structure diagram of the visual sensor.

2.1.2. Visual sensor system design

Visual sensor system is of great significance for acquiring satisfactory weld bead images and improving detection precision in layered deposition process. The structure diagram of the visual sensor is shown in Fig. 2. Since the weld pool with high temperatures is still in liquid form under the welding torch, the deposited bead shape is uncertain. Thus, the visual sensor was fixed to the rear of the welding torch, and the minimum distance between the detection position and welding electrode was 18 mm with a certain lag, ensuring a solidified weld bead.

The sensor was composed of a neural-band filter, two neural-density filters, and a CCD camera. The attenuation of both neural-density filters was 99% and 90%, respectively. The selective center band of the narrow-band filter was 650 nm. This is because the deposited weld bead with extremely high temperature mainly emits infra-red radiations. In this case, its morphology can be clearly seen in the image. To obtain perfect weld bead images, a baffle plate was placed between the torch and the sensor for blocking strong arc light reflections.

2.2. Deposited weld bead image processing

A typical weld bead image with eight-bit grey scale is presented in Fig. 3, from which the deposited bead morphology can be clearly

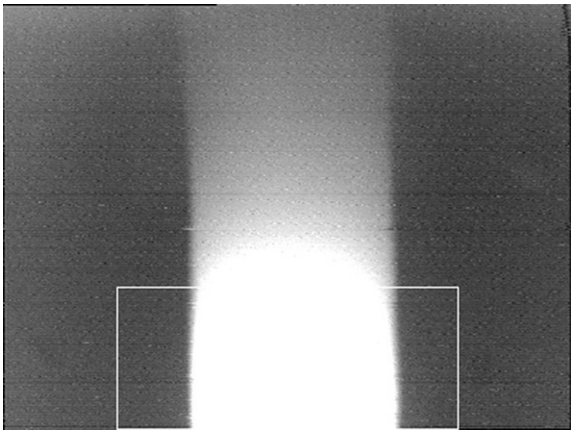

Fig. 3. Typical deposited weld bead image during GMAW-based rapid manufacturing.

seen. For picking up characteristic parameters of the weld bead accurately, a series of corresponding image processing algorithms should be developed. Since the size of the captured image is 400 × 300 pixels, most of the pixels are useless. With a view to saving the CPU time, pixels located in the thin white box were manually selected for image processing, as shown in Fig. 3.

As the GMAW arc has a wide range of wavelengths, the narrow-band filter cannot block all the noises, such as arc light or welding spatter. Furthermore, during the acquisition of images, electro-magnetic noises cannot be avoided, and a long transmission line results in a decrease of signals. Therefore, a weighted average filter, following the two-dimensional Gaussian distribution, was designed to deal with those noises. The principle of this approach is that pixels far from the central pixel have less contribution to filtering results (Baxes, 1994). In this study, a Gaussian template with 3 × 3 size was employed to smooth the image.

The next step is to pick up the bead width from the image. An edge detection method was used to enhance the profile of the image so that the edge can be easily recognized. The principle of the edge detection is mainly based on grey scale between various pixels (Marr and Hildreth, 1980). The edge detection using Laplacian operator is described as follows:

$$\nabla^2 f(i,j) \approx f(i,j) - \frac{1}{4}[f(i,j+1) + f(i,j-1) + f(i+1,j) + f(i-1,j)] \tag{1}$$

where $\nabla^2 f(i,j)$ is the Laplacian operator, $f(i,j)$ is the grey scale located at ith row and jth column, respectively.

After extracting the edge points of the bead width through the Laplacian operator, these points were used for linear fitting. Considering noises produced by the least square method, a Hough transform was employed (Yang et al., 2007). The most important advantages of the Hough transform are its strong anti-noise ability and detection of fitting curve under the condition of low signal-to-noise ratio. It is an approach of mapping the parameter in the xy plane into the Hough plane $\rho\theta$, as expressed in equation (2):

$$x\cos\theta + y\sin\theta = \rho \tag{2}$$

where x and y are coordinate axes in the rectangular coordinate system, ρ and θ are coordinate axes in the Hough plane.

A series of digital image processing procedures, such as the weighted average filter, the Laplacian operator and the Hough transform, were applied to process the bead image, as seen in Fig. 4. The cost of CPU time for the image processing algorithms is less than 20 ms, satisfying the requirement of real-time detection.

2.3. Calibration

The calibration of the visual sensor is a critical issue. The reason is that both the torch and visual sensor are changing their positions vertically. Many process experiments have shown that during the deposition of single-bead multi-layer parts, the deposited bead height decreases during the first four layers before the process is stabilized. Therefore, the height for each layer can be recorded. In future studies, we plan to research the relationship between the stabilized bead height and welding parameters. During the layered deposition process, the welding torch moves with an increment in Z-direction corresponding to the recorded height. In such a circumstance, the distance between the top layer and the camera is almost kept constant. Although the welding speed is slightly adjusted in the closed-loop control system, this will not affect the calibration results. The influence of the welding speed on bead width is much larger than that on bead height (Xiong et al., 2012). In this study, a stainless steel ruler was employed to simply calibrate the visual sensor system. Fig. 5 shows the measured and calculated bead widths during the disposition process. The maximum relative error is approximately 6%.

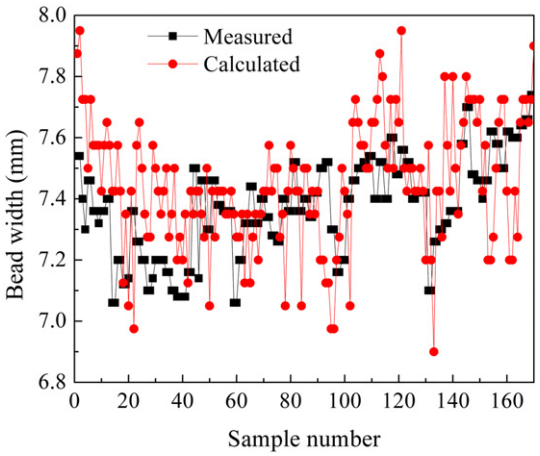

Fig. 5. Measured and calculated values of bead width.

2.4. Design of neural self-learning controller with summational separation

The GMAW-based additive manufacturing is a multi-parameter coupled process, which is complicated, nonlinear and dynamically changing. It is particularly important to choose an appropriate controller. The conventional proportional integral differential (PID) and fuzzy controller cannot meet the requirements due to lack of self-adaptability. Algorithms of the adaptive controller are complex. Consequently, a neural self-learning proportional summational differential (PSD) controller was developed for bead width control. The primary characteristic of the PSD controller is its adaptability of main parameters. Measuring errors between the practical and desired outputs, the PSD can perform adaptive control of the process.

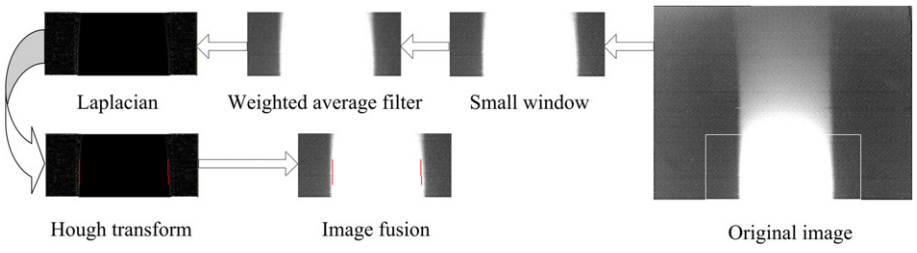

Fig. 4. Procedure of image processing for deposited bead width.

A neural self-learning PSD controller (Marsik, 1983) can be expressed as:

$$\Delta u(t) = K\sum_{i=1}^{3}\varpi_i(t)x_i(t) \tag{3}$$

where $\Delta u(t)$ is the controller output, $x_i(t)$ (i = 1,2,3) are the input signals.

$x_i(t)$ is calculated as follows:

$$\begin{cases} x_1(t) = e(t) - e(t-1) \\ x_2(t) = e(t) \\ x_3(t) = e(t) - 2e(t-1) + e(t-2) \end{cases} \tag{4}$$

$\varpi_i(t)$ can be expressed as:

$$\varpi(t) = \frac{\omega_i(t)}{\sum_{i=1}^{3}|\omega_i(t)|} \tag{5}$$

$$\begin{cases} \omega_1(t) = \omega_1(t-1) + d_P \mathrm{Ke}(t)x_1(t)\mathrm{sgn}\dfrac{\partial y_{\mathrm{out}}(t)}{\partial u(t-1)} \\ \omega_2(t) = \omega_2(t-1) + d_I \mathrm{Ke}(t)x_2(t)\mathrm{sgn}\dfrac{\partial y_{\mathrm{out}}(t)}{\partial u(t-1)} \\ \omega_3(t) = \omega_3(t-1) + d_D \mathrm{Ke}(t)x_3(t)\mathrm{sgn}\dfrac{\partial y_{\mathrm{out}}(t)}{\partial u(t-1)} \end{cases} \tag{6}$$

where $\omega_i(t)$ is the weight coefficient, d_P, d_I, d_D are learning ratios, K is the proportional coefficient of the neuron, $y_{\mathrm{out}}(t)$ is the measured bead width at time t, and $u(t-1)$ is the control variable at time $(t-1)$.

As discussed in Section 2.1.2, the distance between the detection position and welding electrode was 18 mm with a certain lag. To reduce the overshoot and to keep the stability of the deposition process in such a time-delay system, a new PSD controller with summational separation was designed, which can automatically select appropriate parameters of the sum term. The expression can be written as:

$$\Delta u(t) = K[\varpi_1(t)x_1(t) + \beta\varpi_2(t)x_2(t) + \varpi_3(t)x_3(t)] \tag{7}$$

$$\beta = \begin{cases} 1 & \mathrm{error}(t) \le 0.6 \\ 0 & \mathrm{error}(t) > 0.6 \end{cases} \tag{8}$$

An integrated control system structure is shown in Fig. 6. The error and its changes between the given and determined bead width are control inputs. F is the transfer function in the neuron. s is the weight sum of the inputs. W is the system output. In this research, W_{set} is the given bead width and W_{m} is the measured bead width. The output of the PSD controller is an increment of the welding speed v. Z^{-1} denotes the last output of the controller. The measured bead width is sensed and measured by the visual sensor.

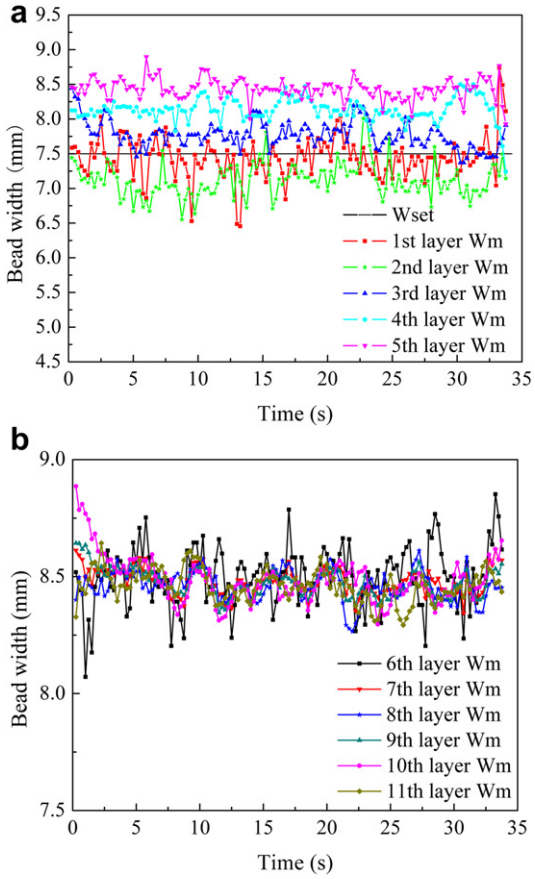

Fig. 7. Bead width measurements of different layers for the 11-layered single bead wall. (a) From first layer to fifth layer, (b) From sixth layer to eleventh layer.

3. Experimental results and discussion

To verify the effectiveness and reliability of the improved PSD controller for bead width control, single-bead multi-pass deposition experiments, divided into two groups, were conducted. Weld beads were deposited on a mild steel substrate of 260 mm × 80 mm × 7.5 mm. H08Mn2Si steel wire was employed as the welding consumable. The welding current was 150 A and the arc voltage was 22 V. Ar (95%) and CO_2 (5%) gas mixture at a constant flow rate of 18 L/min was applied for shielding. Moreover, the initial deposition rate was 5 mm/s.

Single bead walls were fabricated by moving the welding torch along a straight line. All layers were deposited in the same direction. As one layer was deposited, the welding torch was then moved to the beginning of the wall with an increment in Z-direction corresponding to a predefined height. This step was repeated until the whole thin-walled part was completed.

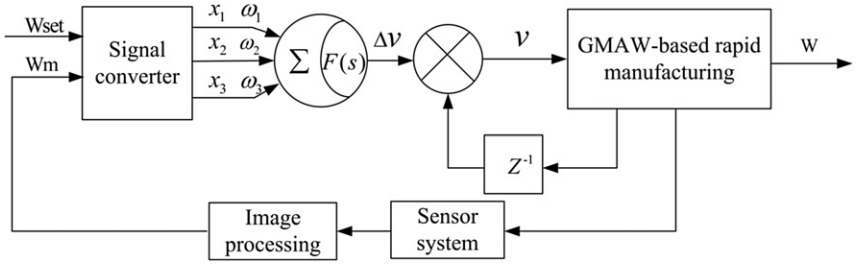

Fig. 6. Neuron self-learning PSD controller for deposited bead width.

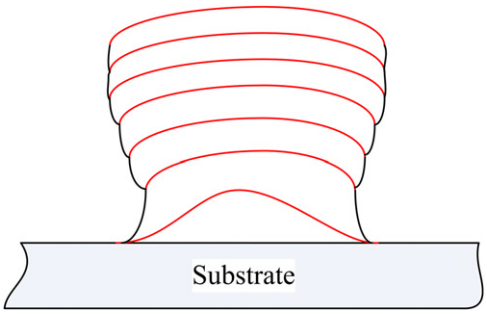

Fig. 8. Deposition model for a thin-walled part.

3.1. Deposition with constant welding speed

To evaluate the improved PSD controller, an eleven-layered single bead wall with constant welding speed (5 mm/s) was deposited for comparison. Fig. 7 shows measured bead widths of the wall. As can be seen in Fig. 7(a), the deposited bead width of the first layer is approximately 7.5 mm. The bead width increases along the deposited layer except for the second layer. The reason for this is that the bead section profile for the first layer can be assumed as a parabola, while it can be regarded as a circle for the second layer, as presented in Fig. 8. The second layer needs more deposition metals. With welding speed remaining constant, the bead width of

Table 1
Error analysis for given and measured bead width.

Deposited layer	Error of deposited bead width	
	Maximum absolute error (mm)	Mean square deviation (mm)
Second	0.902	0.465
Third	0.591	0.239
Fourth	0.434	0.126
Ninth	0.348	0.116
Fourteenth	0.403	0.146
Twenty-first	0.358	0.113

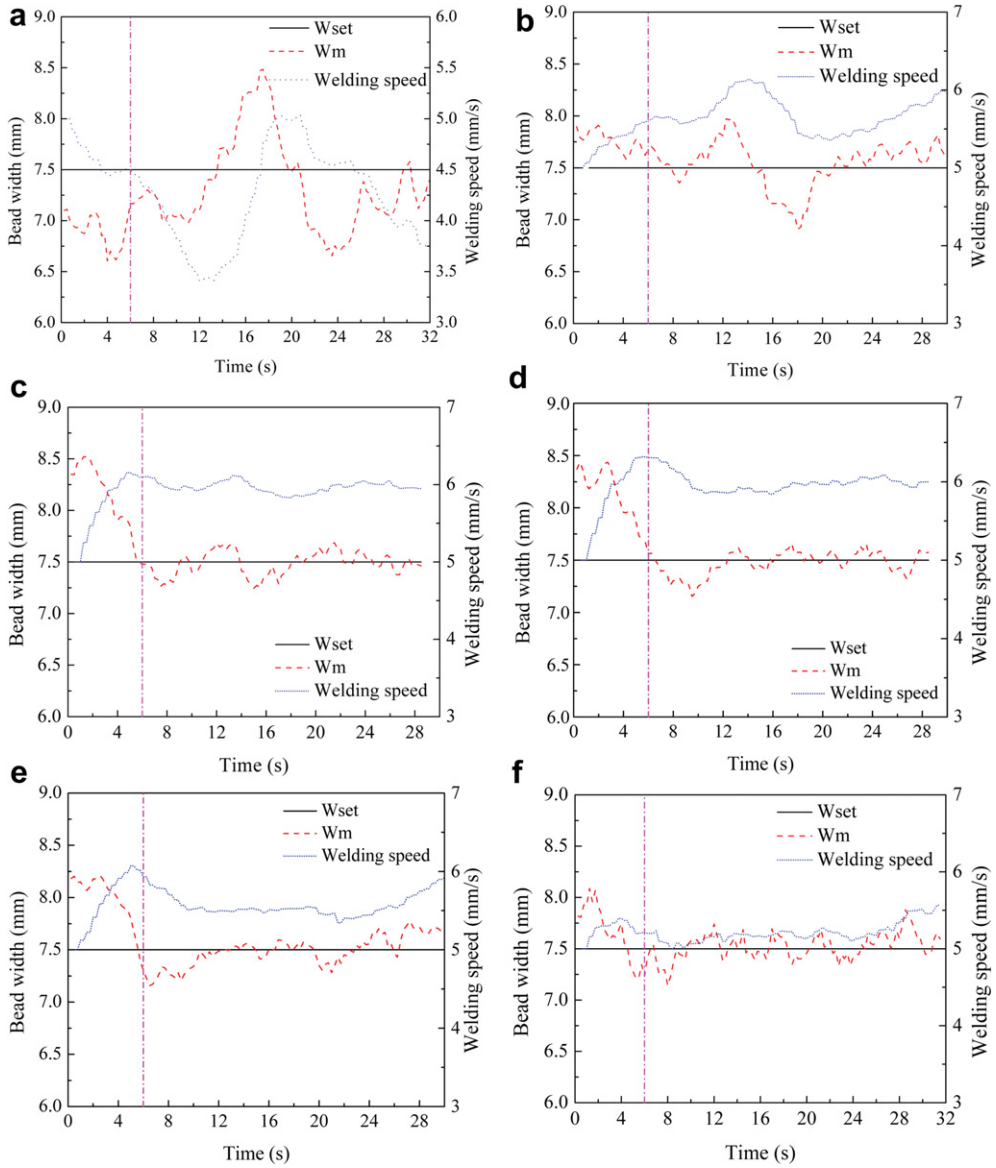

Fig. 9. Curves of neuron self-learning PSD control for deposited bead width. (a) Second layer, (b) Third layer, (c) Fourth layer, (d) Ninth layer, (e) Fourteenth layer, (f) Twenty-first layer.

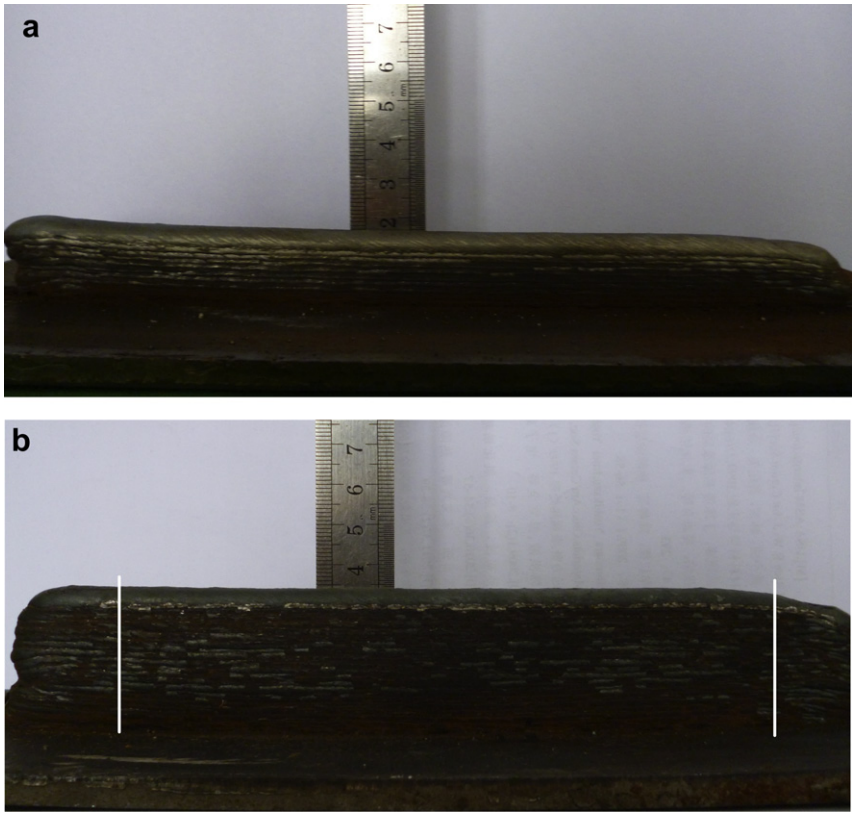

Fig. 10. Multi-layered single bead walls. The lengths of the walls are both 210 mm. (a) Open-loop control, (b) Closed-loop control.

the second layer is relatively low. As the number of deposited layers increases, bad heat-dispersed condition and serious heat accumulation result in an increased bead width. The bead width is stabilized at 8.5 mm due to the balance between the heat loss and heat input.

The control objective is to keep the deposited bead width of the thin-walled part as consistent with that of the first layer, and to compensate for disturbances arising from the previous deposited beads. As discussed in Section 3.1, the bead widths of the deposited layers are larger than that of the first layer, except for the second layer. In the subsequent finishing process, more materials will be removed. As a result of the constant welding speed resulting in excessive heat input, more energy will be consumed.

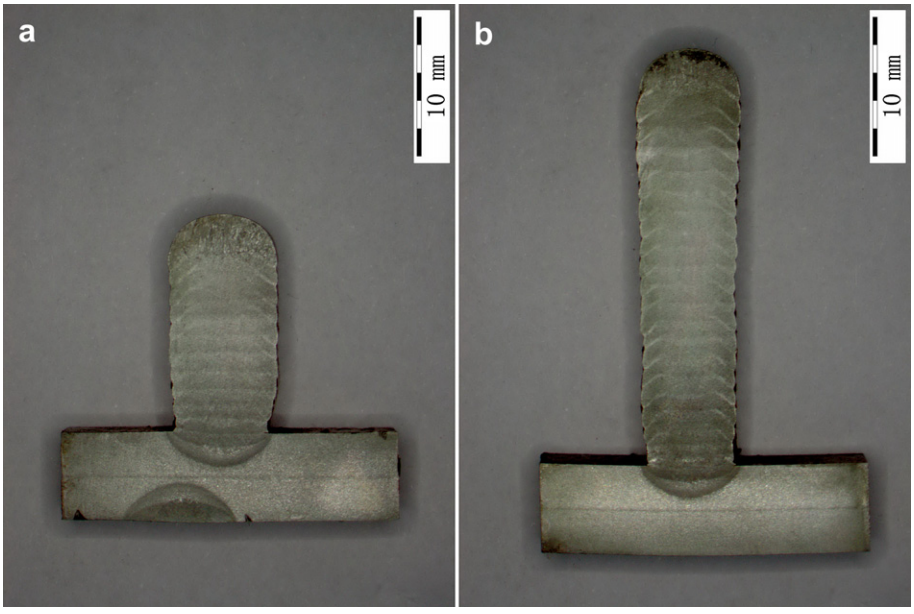

Fig. 11. Cross-sections of the thin-wall parts. (a) Open-loop control, (b) Closed-loop control.

3.2. Deposition with controlling welding speed

In order to reduce material wastes and energy consumptions, heat input of the additive manufacturing process should be adjusted using variable welding speed. A 21-layered thin-walled part was deposited by means of the PSD controller. The varying curves of measured bead width and welding speed for different layers, are shown in Fig. 9. It is worth noting that the initial welding speed for each layer was set as 5 mm/s. The expected bead width for each layer was 7.5 mm. Dash dot lines in the vertical direction, presented in Fig. 9, indicate the dividing lines of the PSD control effect. Curves after the dash dot lines are useful. This is a consequence of the lag distance from the visual sensor system.

As shown in Fig. 9(a), the maximum absolute error is about 0.9 and the mean square deviation is 0.465. Although the bead width fluctuates greatly around the expected bead width, these disturbances can be compensated in a certain degree by the control of subsequent beads. From Fig. 9(b) to Fig. 9(f), it can be seen that the measured bead widths are controlled around 7.5 mm, and no large fluctuations appear, which makes materials saving possible. The welding speed for each layer is larger than 5 mm/s. Other things being equal, heat input in the closed-loop control is less than that in the open-loop control with the welding speed fixing at 5 mm/s. Namely, the reduction of energy consumptions is realized based on the closed-loop control. A detailed error analysis for the given and measured bead width is shown in Table 1. The errors can completely meet the requirement of the GMAW-based layered deposition process.

3.3. Comparisons of material and energy consumption

Photographs of the thin-walled parts are presented in Fig. 10. Note that the PSD controller was turned on at a certain distance after the arc striking points and turned off before the extinguishing points (indicated by the vertical lines in Fig. 10(b)). Fig. 11 shows the macrophotograph of the thin-walled parts.

Table 2 shows the average bead width and welding speed for various layers. The bead widths for different layers are almost consistent by using the improved PSD control system.

The heat input q (J/mm) in the welding process can be expressed as:

$$q = \alpha UI/v \tag{9}$$

where α is the thermal efficiency coefficient, U (V) is the arc voltage, I (A) is the welding current, v (mm/s) is the welding speed.

Supposing that the expected bead width is 7.0 mm, the material wastes in the open-loop control system increase by 10.42% compared with that in the closed-loop control system. The heat input consumptions increase at least by 12.87% in all ten layers.

Table 2
Average bead width and welding speed for different layers.

Layer	Open-loop control		Closed-loop control	
	Average bead width (mm)	Average welding speed (mm/s)	Average bead width (mm)	Average welding speed (mm/s)
Second	7.11	5	7.36	4.19
Third	7.76	5	7.55	5.70
Fourth	8.14	5	7.50	5.95
Fifth	8.44	5	7.49	6.01
Sixth	8.50	5	7.51	5.99
Seventh	8.47	5	7.50	5.86
Eighth	8.46	5	7.54	6.12
Ninth	8.46	5	7.47	5.95
Tenth	8.46	5	7.48	5.88
Eleventh	8.45	5	7.57	5.74

4. Conclusions

This paper aims at decreasing material wastes and energy consumptions in GMAW-based additive manufacturing process. The layered deposition system, with a passive visual sensor and an improved self-learning neuron control of deposited bead width, has been established. The weld bead images were obtained by means of the visual sensor. Corresponding image processing algorithms, including a weighted median filter, a Laplacian operator and a Hough transform, were designed to pick up the characteristic information. An improved neuron self-learning PSD controller was developed to keep the deposited bead widths of various layers consistent. The experiments show that GMAW-based layered deposition process, combining the intelligent detection and control system, is capable of saving materials and energies more than 10% compared with the open-loop control system.

Acknowledgments

This work was supported by National Natural Science Foundation of China, No 51175119.

References

Baxes, G.A., 1994. Digital Image Processing: Principles and Applications. Wiley, New York.
Heralic, A., Christiansson, A.K., Lennartson, B., 2012. Height control of laser metal-wire deposition based on iterative learning control and 3D scanning. Opt. Lasers Eng. 50 (9), 1230–1241.
Jovane, F., Yoshikawa, H., Alting, L., Boer, C.R., Westkamper, E., Williams, D., Tseng, M., Seliger, G., Paci, A.M., 2008. The incoming global technological and industrial revolution towards competitive sustainable manufacturing. CIRP Ann. Manuf. Technol. 57 (2), 641–659.
Karunakaran, K.P., Suryakumar, S., Pushpa, V., Akula, S., 2010. Low cost integration of additive and subtractive processes for hybrid layered manufacturing. Robot. Comput. Integr. Manuf. 26 (5), 490–499.
Marr, D., Hildreth, E., 1980. Theory of edge detection. Proc. R. Soc. Lond. B 207, 187–217.
Marsik, J., 1983. A new conception of digital adaptive PSD control. Probl. Control Inf. Theory 12 (4), 267–279.
Morrow, W.R., Qi, H., Kim, I., Mazumder, J., Skerlos, S.J., 2007. Environmental aspects of laser-based and conventional tool and die manufacturing. J. Clean. Prod. 15 (10), 932–943.
Mughal, M.P., Fawad, H., Mufti, R.A., 2006. Three-dimensional finite-element modelling of deformation in weld-based rapid prototyping. Proc. Inst. Mech. Eng. Part. C J. Eng. Mech. Eng. Sci. 220 (6), 875–885.
Santos, E.C., Shiomi, M., Osakad, K., Laoui, T., 2006. Rapid manufacturing of metal components by laser forming. Int. J. Mach. Tools Manuf. 46 (12–13), 1459–1468.
Song, Y.A., Park, S., 2006. Experimental investigations into rapid prototyping of composites by novel hybrid deposition process. J. Mater. Process. Technol. 171 (1), 35–40.
Spencer, J.D., Dickens, P.M., Wykes, C.M., 1998. Rapid prototyping of metal parts by three-dimensional welding. Proc. Inst. Mech. Eng. Part. B J. Eng. Manuf. 212 (3), 175–182.
Suryakumar, S., Karunakaran, K.P., Bernard, A., Chandrasekhar, U., Raghavender, N., Sharma, D., 2011. Weld bead modeling and process optimization in hybrid layered manufacturing. Comput. Aided. Des. 43 (4), 331–344.
Sutherland, J.W., Gunter, K.L., Haapala, K.R., Khadke, K., Skerlos, S.J., Zimmerman, J.B., Olson, W.W., Sadasivuni, R., 2003. Environmentally benign manufacturing: status and vision for the future. In: NAMRI/SME Transactions, vol. 31. Society of Manufacturing Engineers, Dearborn, MI.
Tang, L., Landers, R.G., 2011. Layer-to-Layer height control for laser metal deposition process. J. Manuf. Sci. Eng. Trans. ASME 133 (2). http://dx.doi.org/10.1115/1.4003691.
Wu, Y., Kovacevic, R., 2002. Mechanically assisted droplet transfer process in gas metal arc welding. Proc. Inst. Mech. Eng. Part. B J. Eng. Manuf. 216 (4), 555–564.
Xiong, J., Zhang, G.J., Hu, J.W., Wu, L., 2012. Bead geometry prediction for robotic GMAW-based rapid manufacturing through a neural network and a second-order regression analysis. J. Intell. Manuf.. http://dx.doi.org/10.1007/s10845-012-0682-1
Yang, S.M., Cho, M.H., Lee, H.Y., Cho, T.D., 2007. Weld line detection and process control for welding automation. Meas. Sci. Technol. 18 (3), 819–826.
Zhang, Y.M., Chen, Y.W., Li, P.J., Male, A.T., 2003. Weld deposition-based rapid prototyping: a preliminary study. J. Mater. Process. Technol. 135 (2–3), 347–357.
Zhang, Y.M., Li, P.J., 2001. Modified active control of metal transfer and pulsed GMAW of titanium. Weld. J. 80 (2), 54–61.
Zhang, Y.M., Liguo, E., Kovacevic, R., 1998. Active metal transfer control by monitoring excited droplet oscillation. Weld. J. 77 (9), 388–395.